J. Fluid Mech. (1997), *vol.* 348, *pp.* 319–325. Printed in the United Kingdom

A note on isolated convection in a rotating two-layer fluid

By DAVID C. CHAPMAN

Woods Hole Oceanographic Institution, Woods Hole, MA 02543, USA

(Received 11 February 1997 and in revised form 10 June 1997)

The approach of Visbeck, Marshall & Jones (1996) is used to explain the primary results of a recent laboratory study of isolated convection in a two-layer fluid reported by Narimousa (1996).

1. Introduction

Recently, Narimousa (1996) has presented the results of some interesting laboratory experiments on isolated convection in a rotating two-layer fluid, as depicted in figure 1. The two-layer fluid was brought to solid-body rotation in a cylindrical tank. Salt water was added at the surface of the upper layer to approximate a constant, uniform, negative buoyancy flux B_0 within a circular region with radius r_0. The water beneath the imposed buoyancy flux became denser and sank to the interface, where it accumulated and produced one of three responses. Sometimes the water became dense enough to penetrate the interface and sink rapidly to the bottom. In other cases, the water remained in the upper layer, forming a density front around the edge of the buoyancy forcing region which slumped radially outward along the interface. The front eventually broke up into mesoscale vortices, but the denser upper-layer water never penetrated the interface. Finally, there were intermediate cases in which the water accumulated at the interface and slowly leaked into the lower layer through 'holes' created in the interface.

Narimousa found that the three regimes could be distinguished by the Richardson number, defined as

$$Ri = g\frac{\delta\rho}{\rho_0}h_0(B_0r_0)^{-2/3}, \tag{1}$$

where $\delta\rho$ is the density difference across the interface, h_0 is the upper-layer thickness, g is gravitational acceleration and ρ_0 is the upper-layer density (see figure 1). If $Ri < 5$, then the convecting dense water penetrated rapidly into the lower layer. If $Ri > 11$, the convecting dense water remained within the upper layer. Intermediate cases occurred for $5 < Ri < 11$. These results were found to be independent of the natural Rossby number, defined by

$$Ro^* = (B_0/f^3h_0^2)^{1/2}, \tag{2}$$

where f is the Coriolis parameter.

Two further interesting findings were reported for the cases which did not penetrate the interface ($Ri > 11$). The resulting vortices had diameters given by

$$D_s \approx 8(B_0r_0)^{1/3}/f \tag{3}$$

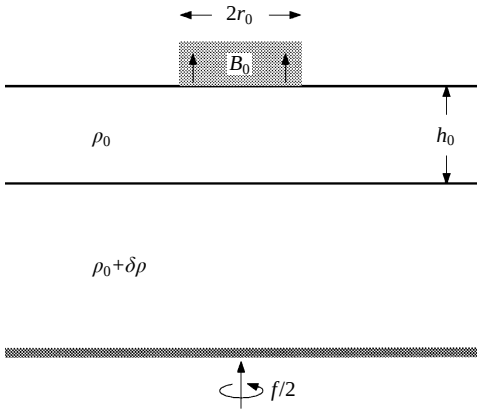

FIGURE 1. Schematic side view of the problem geometry. A negative buoyancy flux B_0 is applied at the surface in a circular region of radius r_0 over a rotating two-layer fluid.

with maximum swirl velocities given by

$$v_s \approx (B_0 r_0)^{1/3}. \tag{4}$$

I offer here an interpretation of Narimousa's results based on the recent 'parcel theory' approach to isolated convection developed by Visbeck, Marshall & Jones (1996; hereinafter referred to as VMJ). The intent is both to provide an explanation for the two-layer laboratory results and to demonstrate the usefulness of the theoretical framework developed by VMJ. I review the VMJ approach in § 2 and apply it to the two-layer fluid in § 3.

2. Theoretical ideas

In virtually all examples of isolated convection, whether numerical calculations or laboratory experiments, the scenario is qualitatively as follows. The water beneath the surface buoyancy flux ($r < r_0$) becomes denser and sinks into the ambient fluid, forming a chimney. The resulting horizontal density gradients established between the chimney water and the ambient water adjust toward geostrophy, generating a rim current flowing around the edge of the chimney. The rim current is baroclinically unstable, so waves grow into eddies which eventually break away from the rim current and exchange chimney water with ambient water.

VMJ assumed that an equilibrium would eventually be reached in which the loss of buoyancy at the surface is balanced by the gain of buoyancy within the chimney produced by eddy exchange with the ambient fluid. By equating these fluxes and choosing appropriate scales for the eddy velocity and density fluctuations, VMJ estimated the equilibrium chimney density anomaly and the time to reach equilibrium in terms of known parameters.

VMJ showed that their estimates are consistent with a wide variety of numerical and laboratory studies of deep convection, in which the ambient stratification is strong enough that the chimney never penetrates to the bottom. They also used their approach to derive scales for shallow convection, in which the ambient stratification is weak and the chimney reaches the bottom rapidly, but they did not report any tests of the shallow convection results.

I have recently tested the approach of VMJ for the case of shallow convection and

found it to be successful in estimating the equilibrium scales (Chapman 1997). It is these results that I apply to the case of isolated convection in a rotating two-layer fluid, as reported by Narimousa (1996). To do so, I consider the inviscid response to a buoyancy flux B_0 applied in a circular region ($r < r_0$) at the surface of a homogeneous fluid with density ρ_0 and constant depth h_0 (i.e. a rigid bottom at depth h_0). The density beneath the buoyancy flux initially increases by an amount

$$\Delta\rho = \frac{\rho_0 B_0}{g h_0} t, \tag{5}$$

where t is time after the buoyancy flux is applied. The rim current produced by this density difference is nearly in thermal wind balance, given by

$$\frac{\partial v}{\partial z} = -\frac{g}{\rho_0 f}\frac{\partial \rho}{\partial r} \approx \frac{g}{\rho_0 f}\frac{\Delta\rho}{R_d}, \tag{6}$$

where v is the velocity along the front, z is the vertical coordinate pointing upwards, r is the radial coordinate directed outward from the centre of the buoyancy forcing, and R_d is the baroclinic Rossby radius, defined by

$$R_d = \left(\frac{g h_0}{f^2}\frac{\Delta\rho}{\rho_0}\right)^{1/2}. \tag{7}$$

The rim current is vertically antisymmetric, so the vertical shear is well approximated by $\partial v/\partial z \approx 2v_m/h_0$ where v_m is the maximum velocity at the surface. Substituting (5), (7) and the approximate vertical shear into (6) produces

$$v_m \approx \tfrac{1}{2}(B_0 t)^{1/2}. \tag{8}$$

My numerical calculations show that this estimate for the maximum velocity within the rim current is quite good (Chapman 1997).

Using (5) and (8) to provide scales in the equilibrium balance assumed by VMJ, the density anomaly at equilibrium and the time to reach equilibrium are estimated as

$$\Delta\rho_e = \alpha^{-2/3}\frac{\rho_0}{g h_0}(B_0 r_0)^{2/3}, \quad t_e = \alpha^{-2/3}\left(\frac{r_0^2}{B_0}\right)^{1/3}, \tag{9}$$

where α represents the efficiency of eddy exchange and is determined from my numerical calculations of shallow convection to be about 0.044 (Chapman 1997). These estimates (9) were first derived by VMJ with the slight difference that they used the total velocity difference ($2v_m$) to define the vertical shear, so their α' is equal to my $\alpha/2$. In summary, $\Delta\rho_e$ is the maximum density increase that the layer of thickness h_0 can experience for the specified buoyancy flux B_0 and radius of forcing r_0. The time to reach this density anomaly is t_e.

A typical example of a numerical calculation of shallow convection is shown in figure 2. A surface buoyancy flux of $B_0 = 16.9 \times 10^{-7}$ m^2 s^{-3} was applied at time $t = 0$ in a circle of radius $r_0 = 20$ km, centred at $x = y = 0$. The water density was initially uniform. The depth $h_0 = 50$ m and Coriolis parameter $f = 1.3 \times 10^{-4}$ s^{-1}. Other details of the primitive-equation model and calculations are presented by Chapman (1997). Horizontal velocity vectors and one density contour (which represents the outermost edge of the denser water) are shown at the surface and bottom, after 5 and 8 days. By day 5, eddies have grown along the rim current and are moving radially outward. By day 8, several eddies have almost separated from the rim current. According to (9), buoyancy equilibration occurs at $t_e = 5.7$ days.

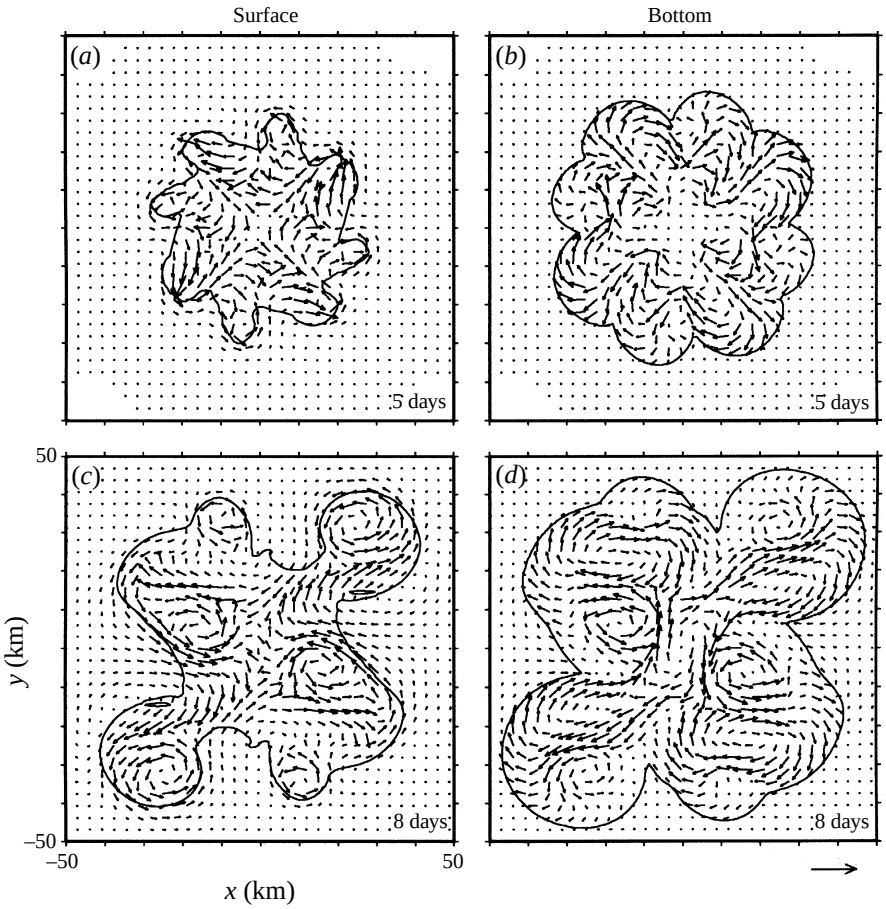

FIGURE 2. Results from a numerical calculation of shallow convection in which a constant surface buoyancy flux of $B_0 = 16.9 \times 10^{-7}$ m^2 s^{-3} is applied over a circular region with radius $r_0 = 20$ km, centred at $x = y = 0$. The depth is $h_0 = 50$ m, and $f = 1.3 \times 10^{-4}$ s^{-1}. Shown are plan views of horizontal velocity vectors (plotted every third grid point) and a density anomaly contour ($\Delta\rho = 0.05$ kg m^{-3}), indicating the outermost edge of the convecting fluid, after (a, b) $t = 5$ days, (c, d) $t = 8$ days of forcing. Left (right) panels are surface (bottom) values. A reference vector of 1 m s^{-1} is plotted in the lower right corner.

3. Application to a two-layer fluid

If the homogeneous fluid of constant depth h_0 in § 2 is imagined to represent the upper layer of the two-layer fluid (figure 1), then $\Delta\rho_e$ represents the density increase possible in the upper layer. If $\Delta\rho_e < \delta\rho$ then the upper-layer density will never become greater than the lower-layer density, despite continued buoyancy forcing, so convection cannot penetrate to the lower layer. If $\Delta\rho_e > \delta\rho$, then the density beneath the buoyancy forcing becomes greater than the lower-layer density before equilibrium is reached, so the convecting fluid penetrates through the interface and to the bottom. The transition between the two situations occurs when $\Delta\rho_e \approx \delta\rho$, which can be written in terms of a transition Richardson number, using (1) and (9), as

$$Ri_T = g\frac{\delta\rho}{\rho_0}h_0(B_0 r_0)^{-2/3} = \alpha^{-2/3} = 8. \tag{10}$$

If $Ri < Ri_T$, then $\Delta\rho_e > \delta\rho$ and convection should penetrate into the lower layer. If $Ri > Ri_T$, then $\Delta\rho_e < \delta\rho$ and convection should not penetrate into the lower layer. This transition ($Ri_T = 8$) is precisely in the middle of the intermediate regime found by Narimousa (1996), suggesting that the transition in the laboratory experiments may be understood in terms of the simple ideas presented in § 2. The intermediate regime occurs for cases close to the transition ($\Delta\rho_e \approx \delta\rho$; $Ri \approx 8$) which are problematic for the theory because the density of the convecting fluid in the upper layer becomes comparable to that in the lower layer, so the interface is presumably displaced appreciably and the simple analysis based on a rigid bottom at depth h_0 is inappropriate. Nevertheless, the conceptual approach of VMJ appears to explain the basic nature of the laboratory results. Furthermore, the transition (10) depends only on Ri and not Ro^*, also in agreement with the laboratory results.

For cases in which convection does not penetrate through the interface ($Ri > 8$), the maximum swirl velocity in the eddies should be approximately the surface velocity of the rim current given by (8) because the eddies develop from the rim current. The swirl velocity is presumably set while the unstable waves are growing, which must occur before equilibrium, i.e. $t < t_e$, but the precise time is uncertain. An upper bound on the swirl velocity can be estimated by evaluating the velocity at equilibrium, i.e. (8) evaluated at t_e,

$$v_e = \tfrac{1}{2}\alpha^{-1/3}(B_0 r_0)^{1/3}. \tag{11}$$

This has the same form as Narimousa's result (4), but with a larger coefficient (1.4 for $\alpha = 0.044$ compared to 1), as it should for an upper bound. If the velocity scale is set at $t \approx t_e/2$, then the coefficient in (11) is reduced to 1, in agreement with Narimousa's results. For the example shown in figure 2, (11) produces $v_e = 0.46$ m s^{-1}, while Narimousa's result (4) suggests $v_s = 0.32$ m s^{-1}. The actual maximum velocities within the eddies in figure 2 range from about 0.3 to 0.4 m s^{-1}, encompassing the estimates reported by Narimousa.

An estimate of the diameter of the eddies does not follow directly from the approach of VMJ. It is clear that the diameter must scale with the baroclinic Rossby radius, but the proportionality factor is unknown. VMJ hypothesized that the diameter should be twice the Rossby radius, in accord with baroclinic instability theory. However, Spall (1995) showed that eddies generated by baroclinic instability at a narrow front increase in size as they move away from the front, making $D \approx 2\sqrt{2}R_d$. Such growth can be seen in figure 2 as the eddies move away from the rim current. Another estimate comes from Saunders' (1973) laboratory result that the number of eddies around the forcing region is given by $m = 1.8 r_0/R_d$. The m eddies must fit around the circumference of the forcing region, so

$$D = 2\pi r_0/m = 2\pi R_d/1.8 = 3.5R_d. \tag{12}$$

Using these estimates and the Rossby radius at equilibrium (i.e. R_d from (7) evaluated using $\Delta\rho_e$ from (9)) with $\alpha = 0.044$ produces

$$D \approx (8 - 9.9)(B_0 r_0)^{1/3}/f. \tag{13}$$

This has the same form as Narimousa's result (3) and also encompasses his estimated coefficient. Furthermore, the larger coefficient of 9.9 falls within the scatter of eddy diameters in Narimousa's figure 7, so the difference may not be meaningful. The diameter predicted by (13) for the example shown in figure 2 is $D = 20$–25 km, which is a good estimate for the larger eddies in the lower panels. Given the uncertainties in defining both the maximum swirl velocity and the diameter of the eddies, it

appears that the laboratory results are again quite consistent with the theoretical ideas presented above.

4. Discussion

Taken together, the above results provide an explanation for the primary findings of Narimousa (1996) in his study of isolated convection in a rotating two-layer fluid. More importantly, they suggest that the parcel theory approach of VMJ represents a powerful framework for understanding problems of this type. For example, the simple scaling expressions might prove to be useful for parameterizing dense water formation in large-scale numerical models, thereby reducing the need for numerous expensive high-resolution calculations.

The results also have implications for the maintenance of the Arctic halocline and the fate of dense water formed by atmospheric cooling and/or brine rejection during ice formation. It is generally thought that the Arctic halocline is maintained by lateral input of dense water from the Arctic shelves where ice production is highest (e.g. Aagaard, Coachman & Carmack 1981). An estimate of the expected maximum increase in density over the shelves can be made using (9). For a shallow coastal polynya with $h_0 = 50$ m and a horizontal scale of $r_0 = 20$ km (e.g. Pease 1987), a typical buoyancy flux of $B_0 = 3 \times 10^{-7}$ m^2 s^{-3} yields $\Delta\rho_e = 0.54$ kg m^{-3}. This density increase is certainly not enough to penetrate the halocline in the deep basins, where the density increases fairly sharply by 3–4 kg m^{-3}. Even a more extreme buoyancy flux of $B_0 = 8 \times 10^{-7}$ m^2 s^{-3} (e.g. Cavalieri & Martin 1994) only increases $\Delta\rho_e$ to 1.04 kg m^{-3}. If the formation region were shallower, say $h_0 = 25$ m, then $\Delta\rho_e$ would double, but this still only approaches the density change through the halocline. Thus, under ordinary circumstances, dense water formed in coastal polynyas may help maintain the halocline by providing cold high-salinity water, but it would not be expected to contribute much to the deep water.

The small values of $\Delta\rho_e$ support the idea that the ambient density of shelf water when freezing begins in coastal polynyas is a very important factor in determining whether or not any dense water is formed on the shelves, as suggested by Melling (1993). If autumn salinities near the coast are slightly lower than normal, then the small increase in density produced in the polynyas may not be enough to cause the surface waters to sink to the bottom. In this case, the formation of dense water would be completely inhibited for that year.

Finally, the simple ideas presented here point out the need for *a priori* theoretical estimates of both the eddy efficiency α and the time at which the velocity scale is set. At present, these are determined empirically, which adds some uncertainty to the general application of the results.

I thank Glen Gawarkiewicz and an anonymous reviewer for several helpful suggestions. I am grateful for the financial support provided by the National Science Foundation (NSF) as part of the Arctic Systems Science (ARCSS) program which is administered through the Office of Polar Programs (grant OPP-9422292).

REFERENCES

Aagaard, K., Coachman, L. K. & Carmack, E. 1981 On the halocline of the Arctic Ocean. *Deep-Sea Res.* **28A**, 529–545.

Cavalieri, D. J. & Martin, S. 1994 The contributions of Alaskan, Siberian, and Canadian coastal polynyas to the cold halocline layer of the Arctic Ocean. *J. Geophys. Res.* **99**, 18343–18362.

CHAPMAN, D. C. 1997 Setting the scales of the ocean response to isolated convection. *J. Phys. Oceanogr.*, in press.

MELLING, H. 1993 The formation of a haline shelf front in wintertime in an ice-covered arctic sea. *Cont. Shelf Res.* **13**, 1123–1147.

NARIMOUSA, S. 1996 Penetrative turbulent convection into a rotating two-layer fluid. *J. Fluid Mech.* **321**, 299–313.

PEASE, C. H. 1987 The size of wind-driven coastal polynyas. *J. Geophys. Res.* **92**, 7049–7059.

SAUNDERS, P. M. 1973 The instability of a baroclinic vortex. *J. Phys. Oceanogr.* **3**, 61–65.

SPALL, M. A. 1995 Frontogenesis, subduction, and cross-front exchange at upper ocean fronts. *J. Geophys. Res.* **100**, 2543–2557.

VISBECK, M., MARSHALL, J. & JONES, H. 1996 Dynamics of isolated convective regions in the ocean. *J. Phys. Oceanogr.* **26**, 1721–1734 (referred to herein as VMJ).